

# A percolation model of semiconductor gas sensors with a hierarchical pore structure

I.A. Pronin<sup>1,\*</sup>, N.D. Yakushova<sup>1</sup>, I.A. Averin<sup>1</sup>, V.A. Moshnikov<sup>2</sup>, B.V. Donkova<sup>3</sup>, D.Tz. Dimitrov<sup>3</sup>, A.Ts. Georgieva<sup>4</sup> and S.S. Nalimova<sup>2</sup>

<sup>1</sup>Department of Nano- and Microelectronics, Penza State University, Penza 440026, Russia

<sup>2</sup>Department of Micro- and Nanoelectronics, Saint-Petersburg Electrotechnical University, Saint-Petersburg 197376, Russia

<sup>3</sup>Laboratory of Nanoparticle Science and Technology, Department of General and Inorganic Chemistry, Faculty of Chemistry and Pharmacy, University of Sofia, Sofia 1164, Bulgaria

<sup>4</sup>Department of Materials Science& Engineering, University of Florida, Gainesville, FL 32611, USA

## Abstract

A percolation model of gas sensors is proposed, on the basis of which the effect of material porosity, pore size and pore size distribution on the gas detection threshold is analyzed. It is shown that micropores exert the greatest influence on gas sensitive properties. An increase in the percolation threshold leads to an increase in the detection threshold of reducing gases. The developed percolation model is used to explain high sensitivity values of sensor structures obtained by the chemical co-precipitation method.

**Keywords:** gas sensor, percolation, sol-gel method, fractals, hierarchical structures.

Received on 01 April 2018, accepted on 28 January 2019, published on 05 February 2019

Copyright © 2019 I.A. Pronin *et al.*, licensed to EAI. This is an open access article distributed under the terms of the Creative Commons Attribution licence (<http://creativecommons.org/licenses/by/3.0/>), which permits unlimited use, distribution and reproduction in any medium so long as the original work is properly cited.

doi: 10.4108/\_\_\_\_\_

\*Corresponding author. Email: Pronin\_i90@mail.ru

## 1. Introduction

Modern chemo-resistive gas sensors consist of nanocrystalline grains of oxide semiconductors, the size of which is usually 2-200 nm [1 – 5]. Currently, the main direction of research is the use of such semiconductor materials with a hierarchical architecture. They are promising for manufacturing of a new generation of multisensor systems and sensors designed for detection of ultra-small concentrations of analyte gases (toxic, narcotic, explosives, etc.) [6 – 15].

At present, when considering nanoobjects, they are generally classified into 0, 1, 2, 3-dimensional and fractal structures. Hierarchical porous structures can arise in the range of 1-100 nm due to the processes of self-organization and self-assembly. Physically, this is due to the tendency of the system to reduce the surface free energy, as well as the possibility of the existence of objects in highly non-equilibrium states. Certainly, a future progress in this area is

connected with the study of techniques that allow self-assembly controlling while finding the system near the bifurcation point.

One of the simplest models of self-assembly products is the Julienne model [16] with the Hausdorff-Besicovitch dimension equal to  $\ln 13 / \ln 3$  in a three-dimensional space. This simplified model schematically reflects the organization of porous materials. It does not consider the nature of the forces responsible for the assembly in various conditions. Nevertheless, it gives the opportunity to compare various functional pores' roles in materials, on the basis of which modern instruments and devices are being created, including ones of ultrahigh sensitivity [17, 18]. Macropores can serve for feeding the analyzed gas and for the output of products of chemical reactions. Micropores, apparently, participate in adsorption processes and chemo-resistive effects in semiconductor gas sensors. In lattice patterns, the existence of a micropore system gives the possibility to block or remove the conductivity. Based on the above, the appearance of percolation clusters and change of the

percolation threshold in porous hierarchical structures is of great practical interest.

The operating principle of chemoresistive gas sensors is the change in the concentration of free charge carriers in a semiconductor during the chemisorption of gases having oxidizing or reducing properties [1 – 4]. As a rule, with a decrease in the average size of the crystallites of the gas sensitive layers, the sensor sensitivity usually will increase. However, simultaneously with this, the detection threshold of analyte gases increases, below of which the sensor does not recognize the analyzed samples. This effect is associated with percolation phenomena in the material and the accompanying conductor-dielectric transition [19 – 22]. The same phenomena can contribute to the occurrence of extremely high sensitivity values (more than  $10^5$ ) of gas sensors operating at the threshold of percolation.

In real hierarchical materials, the analysis of percolation processes is complicated by the existing pore system of various sizes, which play various functional roles. Therefore, the study of influence of the pore size distribution law on the size detection threshold of analyte gases is of particular interest, since modern molecular design technologies make it possible to produce the composites with pores of controlled and reproducible size in a wide range. Thus, the problem of calculating the detection threshold of gases by a sensor is closely related to the problem of percolation threshold  $p_c$  calculating in a material with a hierarchical pore system. The main goal of the paper is a model study of the influence of pore size distribution on the percolation threshold in a semiconductor material. Currently, such data are not available in publications.

## 2. Calculations

To achieve the goal, an original specialized program has been developed in the Delphi environment [23]. A planar square lattice is chosen for modeling, with either a semiconductor crystallite of  $2r$  diameter, or a pore placed in each node. Since a percolation cluster at the percolation threshold exhibits self-similarity properties, than the size of the unit cell does not affect the derivations [24]. Nevertheless, further reasoning is carried out within the framework of the flat zones model, i.e. depletion or enrichment occur throughout the grain. This situation is realized under the condition  $r \ll L_D$ , where  $L_D$  is the Debye screening length, the value of which is tenths of a micrometer in the materials under investigation. Therefore, the simulation is limited to a grain diameter of 1-2 nm, which allows us to consider the smallest pores as micropores. Simultaneously, larger pores will fall into the meso- and macropores' range.

Let's consider the interaction of a sensitive layer of a selective gas sensor with a reducing gas. The oxygen molecules present in the environment in high concentrations ( $> 20\%$ ) will be adsorbed along with the analyzed gas on the sensor surface. Depending on the temperature during adsorption on the oxide surface, the oxygen molecule can dissociate into atoms and acquire a negative charge by

grasping one or two electrons from the oxide conduction band. Formed oxygen ions can play an important role in chemical reactions on the surface of a gas-sensitive oxide layer. The molecules of the reducing gas, on the other hand, acquire a positive charge due to the fact that during adsorption on the surface of the layer one electron passes into the conduction band of the semiconductor oxide. In this case, the number of free electrons  $n_{eff}$  belonging to the grain of the sensory layer can be calculated by the formula:

$$n_{eff} = \frac{4}{3}\pi r^3 n_0 - (4\pi r^2 - k)(N_0 - N_{red}), \quad (1)$$

where  $r$  is the grain radius [cm];  $n_0$  is the concentration of intrinsic charge carriers in the semiconductor [cm<sup>-3</sup>];  $N_0$  is the surface density of chemisorbed oxygen [cm<sup>-2</sup>];  $N_{red}$  is the surface density of the chemisorbed reducing gas [cm<sup>-2</sup>];  $k$  is the coefficient that takes into account the decrease in the effective surface area due to the influence of neighboring grains, surface imperfections, etc. [cm<sup>2</sup>]. An analysis of (1) makes it possible to consider three cases:

- $n_{eff} \geq 1$ . In this case, all the grains are conductive, and the resistance of the layer will vary in proportion to the concentration of the analyzed reducing gas.
- $n_{eff} \leq 0$ . In this case, there are no free charge carriers in the grains, and the gas-sensitive element is a dielectric. Accordingly, the resistance of the layer will not change below a certain concentration of the reducing gas. In this case, the detection threshold is reached.
- $0 < n_{eff} < 1$ . In this case,  $n_{eff}$  value can be considered as the  $p$  probability of the existence of at least one free electron inside the grain.

In the latter case, the sensory structure will be conductive only when the fraction of the conductive  $p$  grains will be equal to the  $p_c$  percolation threshold or above it ( $p \geq p_c$ ). Even with a qualitative analysis of the condition  $0 < n_{eff} < 1$ , it can be seen that the surface density of the chemisorbed reducing gas for small size grains (1-2 nm) can vary by an order of magnitude, as  $n_{eff}$  increases from 0 to 1. Consequently, the detection threshold can also vary over a wide range. Therefore, the determination of the percolation threshold is an important task in the field of gas sensors' research, and the percolation model makes it possible to explain the features of gas sensitivity at ultralow concentrations of detectable gases.

The percolation threshold values are determined for all types of primitive lattice [27-28], but they do not take into account a hierarchical structure of the pores, which is the main feature of gas sensitive layers. A typical structure of a gas sensitive material with a hierarchical pore structure obtained by the sol-gel method is shown in Fig. 1.

It was experimentally established [25] that the main contribution to the porosity of such materials is made by micropores of less than 2 nm, whose fraction is by 2-3 orders of magnitude greater than the pores of all other types (meso- and macropores). Since different types of pores play a different functional role, the influence of pore size distribution on the percolation threshold is determined.

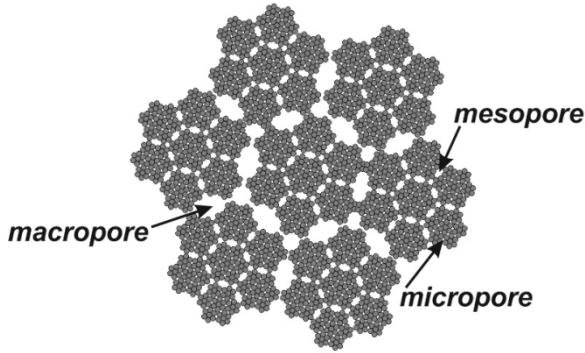


**Figure 1.** A simplified model of self-assembly products (Julienne fractal)

When developing mathematical models for determining the percolation threshold, the following assumptions were made:

- the investigated crystal lattice is flat;
- there are no tunnel transitions through potential barriers;
- charge carriers cannot overcome the existing potential barriers.

The program developed by the authors [23] makes it possible to calculate the percolation threshold  $p_c$  for porous square lattice of arbitrary size and various porosity. Types of pores are divided into several ranks. The pores of the first rank are due to the absence of grains at the corresponding point of the lattice. The pores of the second, third and higher ranks are empty places containing four, nine, etc. points of the lattice.

The percolation threshold, determined only by the pores of the  $i$ -th rank, is denoted as  $p_{ci}$ . The total porosity of the  $\omega$  structure in this case corresponds to the pentagonal fraction of the  $i$ -th rank pores,  $\omega_i$ . The obtained  $p_{ci}$  results for various  $\omega_i$  are used to calculate the percolation threshold  $p_c$  of hierarchical porous structures with different pore size distributions. The total porosity  $\omega$  for materials of this type is the sum of the pore volume fractions of the  $i$ -th rank, i.e.:

$$\omega = \sum_i \omega_i \quad (2)$$

The value of the percolation threshold for various pore size distributions can be obtained by the sum of the values of the percolation thresholds obtained for lattice containing pores of the  $i$ -th rank multiplied by the volume fraction of pores of the corresponding rank:

$$p_c = \sum_i \omega_i p_{ci}(\omega_i) \quad (3)$$

### 3. Results and discussion

Fig. 2 shows the results of percolation threshold simulation for a flat square lattice of  $100 \times 75$  with a porosity of 0 to 35%, containing pores of a certain  $i$ -th rank. The values of the percolation threshold are determined as the average of

20 experiments. Approximation was carried out by the method of least squares.

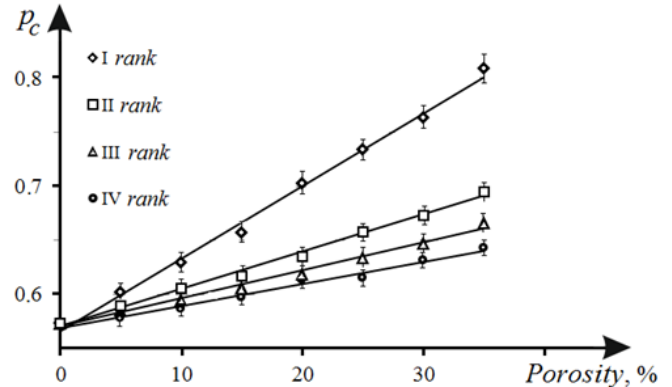


**Figure 2.** Influence of the pore rank and porosity on the percolation threshold

The value of the percolation threshold depends linearly on porosity for pores of all ranks. It is also established that the higher the rank of the pores, the lower the percolation at the same value of porosity.

The effect of the pore size distribution on the percolation threshold is investigated in the presence of different pore ranks in the lattice. The accuracy of determining the percolation threshold for all cases is not less than  $\pm 0.005$ . Table 1 presents the obtained values of the percolation threshold  $p_c$  for lattices with a porosity of 15% and 30% and different pore size distribution laws. Computations are performed according to the four pore distribution laws for each of the two porosity values.

**Table 1.** Dependence of the percolation threshold for various pore size distribution laws with a total porosity of 15 and 30%.

$\omega_1, \%$	$\omega_2, \%$	$\omega_3, \%$	$\omega_4, \%$	$p_c$
Total porosity, $\omega = 15\%$				
85	10	4	1	0.659
25	25	25	25	0.624
10	40	40	10	0.619
1	4	10	85	0.602
85	10	4	1	0.752
25	25	25	25	0.680
10	40	40	10	0.669
1	4	10	85	0.634

It is seen from the results obtained, that the percolation threshold increases with increasing the porosity. The nature of the pore distribution also has a significant effect on the percolation threshold value, which is maximum if the pores of the first rank predominate. In this case, the effect of porosity on the  $p_c$  value is stronger in comparison with the case in which the pores of the fourth rank predominate in the lattice. The results obtained are of interest for the analysis of gas sensitive nanomaterials obtained by the sol-gel technology. It is known that the concentration of micropores

in these materials is by several orders of magnitude higher than the concentration of pores of other types [27]. As it can be seen from Table 1, the effect of porosity on the percolation threshold is particularly high, and the gas detection threshold can be maximally possible for gas sensitive nanomaterials obtained by the sol-gel method with predominated micropores.

Let's consider the effect of porosity and pore size on the detection threshold of reducing gases by sensory structures. Combining (1) and (3), one can obtain the dependence of the surface concentration of the chemisorbed molecules of the reducing gas on the porosity of the sensory structures in the range from 0 to 35%. The calculations were carried out for grains of 1 and 10 nm, having assumed that the structure contained only one rank pores. The obtained dependence is shown in Fig. 3.

It is seen from Fig. 3 that the porosity has a strong effect on the percolation threshold when the grains have a small

size. For example, if the structure contains pores of the first rank and the grain size is 1 nm, the sensitivity threshold increases by almost 20% (with percolation threshold increasing) in the selected porosity range. When the grain size is increased to 10 nm, the above effect becomes insignificant, and the change in the sensitivity threshold is only 1%. However, there is a threshold value for the grain size, below which the sensor will not detect the gas.

The results obtained by the method of mathematical modeling are consistent with the known fact that as the size of semiconductor grains decreases, the sensitivity of sensors and the detection threshold of analyte gases increase.

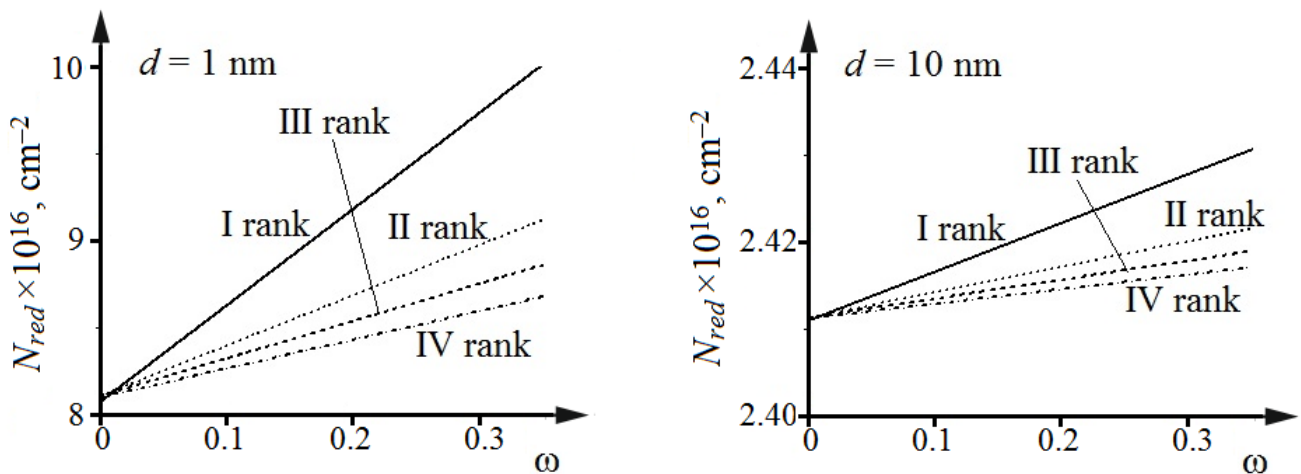


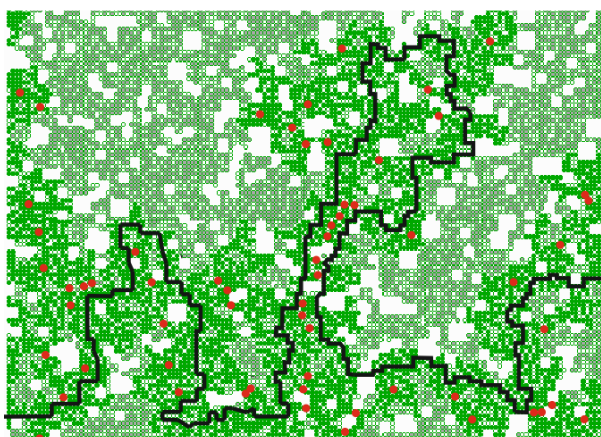
**Figure 3.** Dependence of the surface concentration of chemisorbed molecules of the reducing gas on the porosity of sensory structures

The extension of the obtained model representations allowed explain the high sensor sensitivity values operating at the percolation threshold. Figure 6a shows a porous lattice obtained in the developed program on which a percolating spanning cluster with a structure slightly exceeding the percolation threshold is formed. Red circles in the Figure simulate chemisorbed oxygen forms that deplete individual semiconductor grains and block the flow of electrical current. A solid black line shows the path of least resistance for the flow of electric current. Thus, the length of this broken line actually characterizes the resistance of the structure without the action of the analyte gas possessing reducing properties.

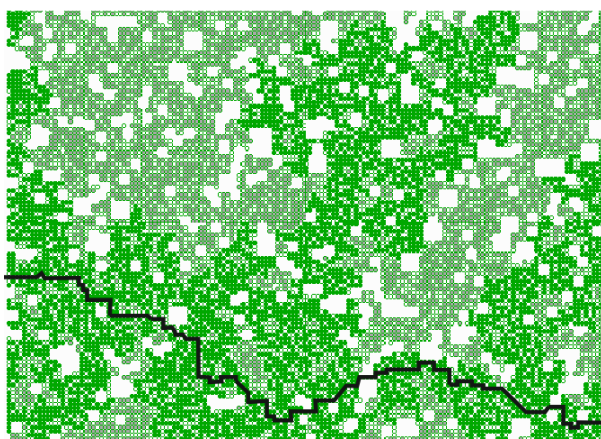
Fig. 4b shows the same structure, but under the action of a reducing gas, which, interacting with chemisorbed oxygen, leads to the removal of the blockade of previously blocked paths. In this case, the broken black line also characterizes the path of least resistance to the

flow of electric current. Thus, this example shows a decrease in resistance by 3-5 times characterized by a ratio of the lengths of broken lines. Obviously, with an infinite increase in the lattice dimensions, the relative change in the resistance of the structure at the percolation threshold is formally unlimited. This explains an ultrahigh sensitivity of sensors with a structure at the percolation threshold.

But it should be noted that when approaching the percolation threshold, the reproducibility of sensor characteristics deteriorates, and the developed devices having the ultrahigh sensitivity will possess individual parameters. This is the main drawback of such sensors, and it is due to the fact that the percolation threshold values will have a wide range for structures of a limited size.



a)



b)

**Figure 4.** The path of least resistance of percolation structures to electric current

Another feature of sensory structures of the percolation type is that the dependence of electric current flow path, and, accordingly, the sensitivity, will depend on unlocking probability of individual adsorption centers. This is illustrated in Fig. 5, where the path of flowing current when blocking certain adsorption centers is shown by the example of the Mandelbrot-Given fractal. If the oxygen-blocked centers occupy another position in the structure, the current path will change, leading to a change in sensitivity.

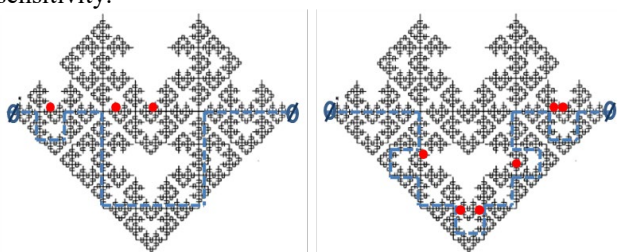


**Figure 5.** Current flow path at various positions of blocked adsorption centers

The developed model concepts are confirmed by the results obtained by the authors [28]. Table 2 presents data on gas sensitivity values of *S* samples of ZnO, Fe<sub>2</sub>O<sub>3</sub>, and

ZnFe<sub>2</sub>O<sub>4</sub> to ethanol and acetone vapors of 1000 ppm concentration.

**Table 2.** Gas sensitivity values of *S* samples of ZnO, Fe<sub>2</sub>O<sub>3</sub>, ZnFe<sub>2</sub>O<sub>4</sub> to ethanol and acetone vapors of 1000 ppm concentration.

Sample	S (ethanol)	S (acetone)
ZNO	35	80
FE <sub>2</sub> O <sub>3</sub>	8	1500
ZNFE <sub>2</sub> O <sub>4</sub>	200	100000

All samples were obtained by chemical co-precipitation out of aqueous solutions of metal salts according to the scheme described in [28]. The structure of all samples is percolating, but the obtained values of gas sensitivity indicate that only in a sample of zinc ferrite a percolating spanning cluster is formed, slightly exceeding the percolation threshold. These data are consistent with the insufficient reproducibility of the structures at the percolation threshold. As it can be seen from the results, the sensitivity of a mixed sample exceeds the sensitivity of individual oxides by 6 times to ethanol, and by 67 times to acetone.

## 5. Conclusion

A percolation model of gas sensors is proposed, on the basis of which the effect of material porosity, pore size and pore size distribution on the gas detection threshold is analyzed. It is shown that micropores exert the greatest influence on gas sensitive properties. An increase in the percolation threshold leads to an increase in the detection threshold of reducing gases. The developed percolation model is used to explain high sensitivity values of sensor structures obtained by the chemical co-precipitation method. The next stage in the development of the model is to take into account not only the percolation thresholds but also the percolation level.

## Acknowledgements.

This work was supported by Ministry of Education and Science of the Russian Federation, projects No. 16.897.2017/4.6; No. MK-1882.2018.8 (Grant of the President); No. CII-84.2018.1 (Scholarship of the President).

## References

- [1] Korotcenkov, G., 2010 *Chemical Sensors, General Approaches Sensor Technology*, Vol 1 (NY: Momentum Press);
- [2] Sun, Y. F., Liu, S. B., Meng, F. L., Liu, J. Y., Jin, Z., Kong, L. T., Liu, J. H., 2012 Metal oxide nanostructures and their gas sensing properties: a review. *Sensors* 12(3): pp. 2610-2631;
- [3] Comini, E., 2006 Metal oxide nanocrystals for gas sensing. *Analytica chimica acta* 568(1): pp. 28-40;
- [4] Wang, C., Yin, L., Zhang, L., Xiang, D., Gao, R., 2010 Metal oxide gas sensors: sensitivity and influencing factors. *Sensors* 10(3): pp. 2088-2106;
- [5] Lashkova, N. A., Permiakov, N. V., Maximov, A. I., Spivak, Y. M., Moshnikov, V. A., 2015 Local analysis of semiconductor nanoobjects by scanning tunneling atomic force microscopy. *St. Petersburg Polytechnical University Journal: Physics and Mathematics* 1(1): pp. 15-23;
- [6] Gracheva, I. E., Moshnikov, V. A., Karpova, S. S., Maraeva, E. V., 2011 Net-like structured materials for gas sensors. *Journal of Physics: Conference Series* 291 (1): pp. 012017;
- [7] Moshnikov, V. A., Gracheva, I., Lenshin, A. S., Spivak, Y. M., Anchkov, M. G., Kuznetsov, V. V., Olchowik, J. M., 2012 Porous silicon with embedded metal oxides for gas sensing applications *J. Non-Cryst. Solids* 358(3): pp. 590-595;
- [8] Zhang, J., Wang, S., Xu, M., Wang, Y., Zhu, B., Zhang, S., Huang, S.M., Wu, S., 2009 Hierarchically porous ZnO architectures for gas sensor application. *Cryst. Growth Des.* 9(8): pp. 3532-3537;
- [9] Liu, J., Guo, Z., Zhu, K., Wang, W., Zhang, C., Chen, X., 2011 Highly porous metal oxide polycrystalline nanowire films with superior performance in gas sensors. *J. Mater. Chem.* 21(30): pp. 11412-11417;
- [10] Huang, J., Wu, Y., Gu, C., Zhai, M., Sun, Y., Liu, J., 2011 Fabrication and gas-sensing proper-ties of hierarchically porous ZnO architectures. *Sens. Actuat. B* 155(1): pp. 126-133;
- [11] Wang, X., Liu, W., Liu, J., Wang, F., Kong, J., Qiu, S., He, C., Luan, L., 2012 Synthesis of nestlike ZnO hierarchically porous structures and analysis of their gas sensing properties. *ACS Appl Mater Interfaces* 4(2): pp. 817-825;
- [12] Fan, F., Tang, P., Wang, Y., Feng, Y., Chen, A., Luo, R., Li, D., 2015 Facile synthesis and gas sensing properties of tubular hierarchical ZnO self-assembled by porous nanosheets. *Sens. Actuat. B*, 215: pp. 231-240;
- [13] Zhang, L., Zhao, J., Lu, H., Li, L., Zheng, J., Li, H., Zhu, Z., 2012 Facile synthesis and ultra-high ethanol response of hierarchically porous ZnO nanosheets. *Sens. Actuators B*, 161(1): pp. 209-215;
- [14] Liu, X., Zhang, J., Wang, L., Yang, T., Guo, X., Wu, S., Wang, S., 2011 3D hierarchically porous ZnO structures and their functionalization by Au nanoparticles for gas sensors. *J. Mater. Chem.* 21(2): pp. 349-356;
- [15] Wang, P. P., Qi, Q., Zou, X., Zhao, J., Xuan, R. F., Li, G. D., 2013 A precursor route to porous ZnO nanotubes with superior gas sensing properties. *RSC Adv.* 3(46): pp. 23980-23983;
- [16] Jullien, R., 1987 *Fractal Aggregates*. *Comm. Cond. Mat. Phys.* 13(4): pp. 177-205;
- [17] Moshnikov, V. A., Gracheva, I. E., Kuznetsov, V. V., Maximov, A. I., Karpova, S. S., Ponomareva, A. A., 2010 Hierarchical nanostructured semiconductor porous materials for gas sensors. *J. Non-Cryst. Solids* 356(37): 2020-2025;
- [18] Gracheva, I. E., Moshnikov, V. A., Maraeva, E. V., Karpova, S. S., Aleksandrova, O. A., Alekseyev, N. I., Kuznetsov, V.V., Olchowik, G., Semenov, K.N., Startseva, A.V., Sitnikov, A.V., Olchowik, J.M., 2012 Nanostructured materials obtained under conditions of hierarchical self-assembly and modified by derivative forms of fullerenes. *J. Non-Cryst. Solids* 358(2): pp. 433-439;
- [19] Ulrich, M., Kohl, C. D., Bunde, A., 2001 Percolation model of a nanocrystalline gas sensitive layer. *Thin Solid Films* 391(2): pp. 299-302;
- [20] Dräger, J., Russ, S., Sauerwald, T., Kohl, C. D., Bunde, A., 2013 Percolation transition in the gas-induced conductance of nanograin metal oxide films with defects. *J. Appl. Phys.* 113(22): pp. 223701;
- [21] Jobmann, M., Billaux, D., 2010 Fractal model for permeability calculation from porosity and pore radius information and application to excavation damaged zones surrounding waste emplacement boreholes in opalinus clay. *International Journal of Rock Mechanics and Mining Sciences* 47(4): pp. 583-589;
- [22] Aroutiounian, V. M., Ghoolinian, M. Z., Tributsch, H., 2000 Fractal model of a porous semiconductor. *Appl. Surf. Sci.* 162: pp. 122-132;
- [23] Averin I.A., Pronin I.A., Karmanov A.A., Karpanin O.V., 2014 Determination of the percolation threshold on a square lattice with a hierarchical pore system. Certificate of state registration of computer programs No. 2014612604;
- [24] Feder, E. 1991 *Fractals*: in Russian (Moscow: Mir);
- [25] Gracheva, I.E., 2009 Semiconductor mesh nanostructured composites based on tin dioxide obtained by sol-gel method for gas sensors. Thesis for a degree of Candidate of Physical and Mathematical Sciences (St. Petersburg State Electrotechnical University "LETI") St. Petersburg. (In Russian);
- [26] Rumyantseva, M.N., 2009 Chemical modification and sensory properties of nanocrystalline tin dioxide. Thesis for a degree of Doctor of Chemical Sciences. Moscow, (In Russian);
- [27] Pronin, I.A., Averin, I.A., Moshnikov, V.A., Yakushova, N.D., Kuznetsova, M.V., Karmanov, A.A., 2014 Percolation model of a gas sensor based on semiconductor oxide nanomaterials with a hierarchical pore structure. *Journal of Nano- and Microsystems Technique* 9: pp. 15–19, (In Russian);

- [28] Moshnikov, V. A., Nalimova, S. S., Seleznev, B. I.,  
2014 Gas-sensitive layers based on fractal-percolation  
structures. *Semiconductors* 48(11): 1499-1503.